

Graft-Interpenetrating Polymer Networks of Epoxy with Polyurethanes Derived from Poly(ethyleneterephthalate) Waste

Saurabh Chaudhary,^{1,2} Surekha Parthasarathy,¹ Devendra Kumar,² Chitra Rajagopal,¹ Prasad Kumar Roy¹

¹Centre for Fire, Explosive and Environment Safety, DRDO, Timarpur, Delhi 110054, India

²Department of Applied Chemistry and Polymer Technology, Delhi Technological University, Delhi 110042, India

Correspondence to: P. K. Roy (E-mail: pk_roy2000@yahoo.com or pkroy@cfees.drdo.in)

ABSTRACT: Polyester polyurethanes derived from poly(ethyleneterephthalate) (PET) glycolysates were blended with epoxy to form graft-interpenetrating networks (IPNs) with improved mechanical properties. Microwave-assisted glycolytic depolymerization of PET was performed in the presence of polyethylene glycols of different molecular weights (600–1500). The resultant hydroxyl terminated polyester was used for synthesis of polyurethane prepolymer which was subsequently reacted with epoxy resin to generate grafted structures. The epoxy-polyurethane blend was cured with triethylene tetramine under ambient conditions to result in graft IPNs. Blending resulted in an improvement in the mechanical properties, the extent of which was found to be dependant both on the amount as well as molecular weight of PET-based polyurethane employed. Maximum improvement was observed in epoxy blends prepared with polyurethane (PU1000) at a loading of 10% w/w which resulted in 61% increase in tensile strength and 212% increase in impact strength. The extent of toughening was quantified by flexural studies under single edge notch bending (SENB) mode. In comparison to the unmodified epoxy, the Mode I fracture toughness (K_{IC}) and fracture energy (G_{IC}) increased by ~45% and ~184%, respectively. The underlying toughening mechanisms were identified by fractographic analysis, which generated evidence of rubber cavitation, microcracking, and crack path deflection. © 2014 Wiley Periodicals, Inc. *J. Appl. Polym. Sci.* **2014**, *131*, 40490.

KEYWORDS: blends; grafting; mechanical properties; polyesters; polyurethanes

Received 25 October 2013; accepted 21 January 2014

DOI: 10.1002/app.40490

INTRODUCTION

The last few decades have seen an enormous increase in the usage Poly(ethyleneterephthalate) (PET) as packaging material, primarily because of its excellent mechanical and barrier properties, low cost, and high energy effectiveness. The largest consumption of this thermoplastic is by the textile sector for production of synthetic fibers, followed by bottling industry for packaging beverages, particularly carbonated drinks.¹ Unfortunately, the large scale usage of PET, in conjunction with irresponsible methods of disposal has led to its accumulation in the environment, for which it has received much criticism by environmentalists.²

Several strategies have evolved for effective management of PET wastes, the most common being the “primary” and “secondary” recycling techniques.³ Although, the last two decades have seen huge advancements in “bottle to fiber and bottle to bottle” recycling technologies,¹ only a fraction of PET is practically recycled, the primary reason being the high cost of the recycled

product.⁴ It is thus highly desirable to adopt technically and economically feasible routes towards recycling of PET into industrially important products. In this context, tertiary recycling of PET offers interesting possibilities.^{5–7} This process refers to the chemical depolymerization of PET, leading to the production of fuels or basic chemicals. The ester linkages which form the backbone of PET can be chemically transformed by processes like glycolysis, aminolysis, hydrolysis, acidolysis, alkalolysis, and alcoholysis, out of which the former two have reached the level of commercial maturity.^{5,7} The polyester polyols formed as a result of glycolytic depolymerization of PET have further been used for preparation of industrially important polymers including polyurethanes,^{8,9} unsaturated polyesters,¹⁰ and UV curable films.¹¹

In our previous papers,^{6,12–14} we have demonstrated the potential of microwave-assisted glycolytic process towards reducing the time and energy requirements towards PET depolymerization. The aromatic polyester polyols obtained by PET glycolysis

Additional Supporting Information may be found in the online version of this article.

© 2014 Wiley Periodicals, Inc.

were used to prepare polyurethane foams with superior mechanical properties as compared with its aliphatic analogs. This was attributed to the presence of aromatic functionalities in the polyurethane main chain.¹⁴ We hypothesize that introduction of PET-derived polyurethanes can result in substantial improvements in mechanical properties of brittle polymers, provided optimized blends are formulated.

In this context, blending of epoxy with elastomeric polyurethanes has been attempted to improve the fracture toughness of the base brittle thermoset.^{15–20} Epoxy-polyurethane blends offer interesting properties, as polyurethanes are associated with excellent elasticity, abrasion resistance, and damping properties, while the epoxy resins possess excellent mechanical properties along with strong adhesion to metals. Polyurethanes are particularly attractive elastomers for toughening purpose, because of the possibility of tailoring its mechanical properties by altering the chemical structure.^{16,21–25} Several attempts in this direction have been made where the polyurethane is derived from poly(oxyethylene),¹⁹ poly(oxytetramethylene),²⁶ poly(caprolactone),²⁷ poly(oxypropylene),¹⁸ castor oil,^{16,20} and polyester polyols.¹⁶ However, the potential of PET glycolysate-based polyurethane has not yet been explored.

In this article, we report the preparation of an epoxy network with aromatic polyester polyurethanes derived from PET wastes by microwave-assisted glycolysis. The reaction of terminal NCO in polyurethane with the hydroxyl groups available with the epoxy resin leads to grafting and subsequent curing of the epoxy resin leads to the formation of graft-interpenetrating networks, with enhanced mechanical properties.²⁸ The primary aim of this work is to improve the energy absorption characteristics of the base epoxy resin by blending with PET-based polyurethanes, and to gain insight into the underlying toughening mechanisms.

EXPERIMENTAL

Materials

Disposed PET bottles were collected, washed, dried, and used after removal of the polyethylene caps and the polypropylene label. The bottles were shredded into small pieces (6 mm × 6 mm) and glycolytic experiments were performed with polyethylene glycol (PEG) of varying molecular weights for which PEG 600, PEG 1000, and PEG 1500 (E. Merck) were used. Zinc acetate dihydrate [Zn (CH₃COO)₂ · 2H₂O, Merck] with a purity of 99% was employed as the trans-esterification catalyst. Metallic carboxylate-based catalyst, Di-butyltinlaurate (DBTL), Diphenylmethane 4,4'-diisocyanate: a mixture of di- and triisocyanates (MDI) was obtained from E. Merck were used without any further purification. Di-glycidyl ether of bis-phenol A epoxy resin (DGEBA) (Huntsman, Araldite GY 250; epoxy equivalent 190 g/eq) and triethylene tetramine (TETA) hardener (HY 951; amine content 32 eq/kg) were used as received.

Microwave-Assisted Glycolysis

Microwave-assisted glycolysis of PET was performed in the presence of glycols of varying molecular weight as per the procedure reported previously.¹³ A domestic microwave oven (LG) with a magnetron source for microwave generation (2.45 GHz,

maximum power: 900 W) was used for this purpose. PET pieces (10 g) together with requisite amount of glycol and zinc acetate (0.5%, w/w, PET) were introduced into a loosely stoppered reaction flask which was placed in the microwave reactor. PET glycolysis was performed at PET : glycol: 1 : 2, and the reaction was allowed to proceed at 450 W for extended time periods. After predetermined periods, the reaction mixture was filtered through a copper wire mesh (0.5 × 0.5 mm² pore size), and the remaining unreacted PET flakes were weighed to quantify the extent of PET conversion, as the ratio of mass of PET reacted to the initial mass of the flakes taken. To obtain the polyol, the reaction mixture was cooled to room temperature, dissolved in a suitable amount of CHCl₃, and shaken vigorously with an equal amount of distilled water in a separating funnel to get rid of the unreacted glycol and zinc acetate catalyst. The organic layer was subsequently collected, and the residual water was removed in a rotary evaporator. The obtained glycolysates were dried over molecular sieve (5A) and stored under desiccation. The obtained polyols will be referred to as PY-*x*, where *x* refers to the molecular weight of glycol used for its preparation. For example, PY-1000 refers to the polyester polyol formed after glycolysis of PET with PEG 1000.

Synthesis of Polyurethane Prepolymer

PET glycolysate-based NCO terminated polyurethanes was prepared by adding requisite amount of diphenylmethane-4,4'-diisocyanate (PET glycolysate : MDI :: 1 : 2) in a round bottom flask in the presence of DBTL as a catalyst. The reaction was performed under inert atmosphere at 15°C, which was maintained using an ice bath. The polyurethane prepolymer obtained will be designated as PU *x*, where *x* refer to the molar mass of glycol used for glycolysis.

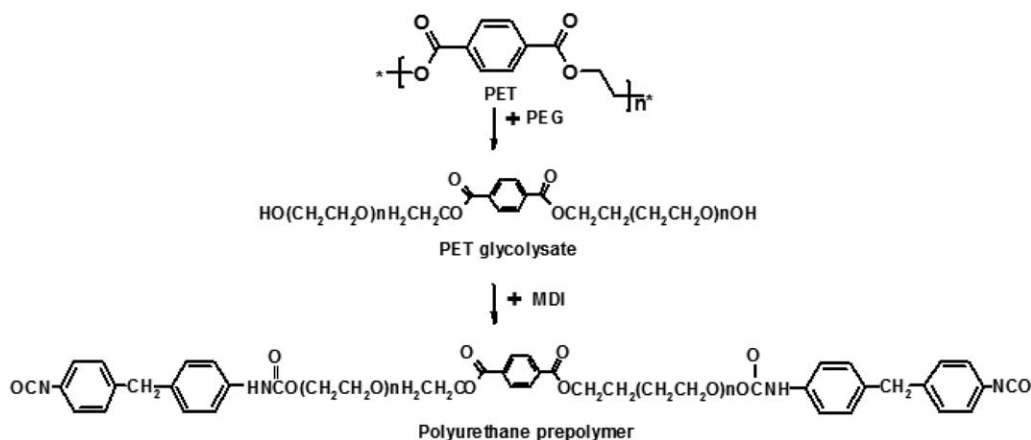
Preparation of Epoxy Blends

The polyurethane prepolymer was added to epoxy resin in varying amounts (5, 10, and 15% w/w) and stirred for 10 min (700 rpm) on a magnetic stirrer under ambient temperature to aid homogenization. TETA hardener was subsequently added and the mixture was degassed to remove entrapped air bubbles and poured into silicone molds for specimen preparation. For comparison purposes, neat epoxy samples were also prepared, which will be referred to as EP. All grafted IPNs prepared in the presence of polyurethanes will be referred to as E_{*y*}PU_{*x*}, where *x* refers to the molecular weight of glycol used for its preparation and *y* refers to the amount of polyurethane in the formulation (% w/w). For example, E10PU600 refers to a blend of epoxy with PU 600 (10% w/w).

CHARACTERIZATION TECHNIQUES

Viscometric Studies

The viscosity-average molecular weight of PET was determined by solution viscometry. Samples were dissolved in a mixture of phenol and 1,1,2,2-tetrachloroethane (60/40 w/w) under heating, and the intrinsic viscosity [η] was measured using Ubbelohde suspension level viscometer at 25°C. The viscosity average molecular weight of PET was calculated using the following equation²⁹:



Scheme 1. Reaction schematic illustrating the formation of PET-derived polyurethane.

$$[\eta] = 75.5 \times 10^{-3} \text{ mL/g} M_v^{0.685} \quad (1)$$

The intrinsic viscosity of the glycolysed polyols was determined in methanol at 25°C.

Hydroxyl Number Estimation

The hydroxyl number (HN) was determined using acetic anhydride, as per test method A, described in ASTM D 4274–99. For the purpose of acid number determination, the solution was titrated against standard methanolic KOH solution in acetone medium, as per the procedure reported previously.

Isocyanate Content

The NCO content was determined by nonaqueous titrimetry as per the established procedure, where the polyurethane was allowed to react with excess dibutylamine under reflux. The amount of unreacted dibutylamine was quantified by titrating against standard hydrochloric acid, which was used to estimate the NCO content in the prepolymer.

Structural Characterization

The FTIR spectra of samples were recorded in the wavelength range 4000–600 cm^{-1} using Fourier Transform Infrared (FTIR) spectroscopy on a Thermo Fisher FTIR (NICOLET 8700) with an attenuated total reflectance (ATR) crystal accessory.

Thermal Characterization

The changes in the thermal properties of the samples were investigated using DSC (TA instruments, Q 20 module) under nitrogen atmosphere. Approximately 4–6 mg of the sample was placed in a 40 μL aluminum cap without pin and sealed with a lid. After erasing the thermal history of samples, they subjected to a heating program from -60 to 250°C at $10^\circ\text{C min}^{-1}$. Thermogravimetric studies were performed using Perkin Elmer Diamond STG-DTA-DSC in N_2 atmosphere in the temperature range of 50 – 800°C . A heating rate of $10^\circ\text{C min}^{-1}$ and sample mass of 5.0 ± 0.5 mg was used for each experiment. Percentage crystallinity was calculated from the DSC traces as follows.

$$\% \text{ Crystallinity} = \frac{\Delta H_{f(\text{observed})}}{\Delta H_{f(100\% \text{ crystalline})}} \times 100 \quad (2)$$

where $\Delta H_{f(\text{observed})}$ is the enthalpy associated with melting of the material and $\Delta H_{f(100\% \text{ crystalline})}$ is the enthalpy of 100%

crystalline PET reported in the literature to be 135.8 J g^{-1} (Ref. 30).

Evaluation of Mechanical Properties

Quasi-static mechanical properties were determined according to ASTM method D638 using a Universal Testing System (International equipments) at ambient temperature. The samples were subjected to a cross head speed of 50 mm min^{-1} . The notched Izod impact strength of the specimens was determined according to ASTM D 256 using an impact strength testing machine (International Equipments, India) at a striking velocity of 3.5 m s^{-1} . Six identical specimens were tested for each composition and the average results along with the standard deviation values have been reported.

Notched flexural testing of the samples was performed under three point single edge notch bending mode according to ASTM D 5045. For this purpose, specimens of requisite dimensions ($127 \text{ mm length} \times 12.5 \text{ mm width} \times 3.5 \text{ mm thickness}$ and 3 mm notch) were prepared and subjected to a deformation rate of 2 mm min^{-1} while maintaining 60 mm span length. The data obtained was analyzed to determine the mode I fracture toughness (K_{IC}) and fracture energy (G_{IC}),³¹ by assuming the Poisson's ratio of epoxy to be 0.35 .³²

Morphological Studies

The surface morphology of samples was studied using a Scanning Electron Microscope (Zeiss EVO MA15) under an acceleration voltage of 20 kV . Samples were mounted on metal stubs and sputter-coated with gold and palladium (10 nm) using a sputter coater (Quorum-SC7620) operating at 10 – 12 mA for 60 s .

RESULTS AND DISCUSSION

Polyester Polyols from PET by Microwave-Assisted Glycolysis

A schematic of the PET glycolytic process, followed by its reaction with isocyanate is presented in Scheme 1. The conditions employed for glycolysis have been discussed in our previous papers.^{12,13} The TG and DSC trace of the PET used for this study is presented in the Supporting Information Figure S1. The PET samples exhibit a sharp melting point peaking at 246°C and undergoes a single step decomposition commencing at 400°C . The DSC crystallinity as determined from the area

Table I. Characteristics of the Glycolysed Polyols

Polyol	HN (mg KOH/g)	$[\eta]$ (dL/g)	M_n	M_w	M_z	PDI
PL 600	110.3 ± 5	0.045	1114	2025	3074	1.8
PL 1000	86.4 ± 4	0.051	1745	3078	4436	1.7
PL 1500	32 ± 3	0.056	2776	4080	5508	1.5

under the endotherm is ~27.2% and the molecular weight (M_n) of PET, as determined from viscometric studies is 27,431. Transesterification of PET resulted in the formation of a viscous liquid, which was soluble in nonpolar organic solvents like CHCl_3 , CH_2Cl_2 , CCl_4 , benzene, toluene, etc. and could be separated from the water soluble reactants and catalyst by water extraction. The maximum level of PET conversion could be achieved within 30 min of irradiation, while under the same PET : glycol concentrations; the reaction takes ~9 h to reach the same level of depolymerization.

Physical Properties of Polyols

The HN of the glycolysed products obtained after the reaction of PET with increasing molecular weight glycols after microwave irradiation for 30 min is listed in Table I. The intrinsic viscosities as determined in methanol at 25°C, along with the M_n , M_w , and M_z values, as obtained by GPC are also presented. It is to be noted that prior to determination of the HN, the liquid sample was extracted with chloroform, to eliminate the contribution of water soluble reactants i.e. PEG and side products, i.e. ethylene glycol, to the HN. As expected, with increasing molecular mass of glycol employed for the transesterification purpose, the intrinsic viscosity and the molecular mass of the resulting polyol increases, while the hydroxyl number decreased.

PET-Derived Polyurethane

The resulting polyester polyols were subsequently reacted with MDI to prepare NCO terminated polyurethane prepolymer (PET glycolysate : MDI :: 1 : 2). The FTIR spectra of PET, a representative glycolysate (PY 1000) and the polyurethane prepolymer obtained there from (PU 1000) is presented in Figure 1. Both PET as well as its glycolysed derivative exhibit absorption band peaking at 1715 cm^{-1} due to carbonyl stretching ($\nu_{\text{C=O}}$). The appearance of a broad absorption band (~3200–3600 cm^{-1}) in the spectra of glycolysed PET can be attributed to the presence of terminal hydroxyl groups. An absorption peak at 2200 cm^{-1} can be seen in the FTIR spectra of PU prepolymer, which can be attributed to the NCO

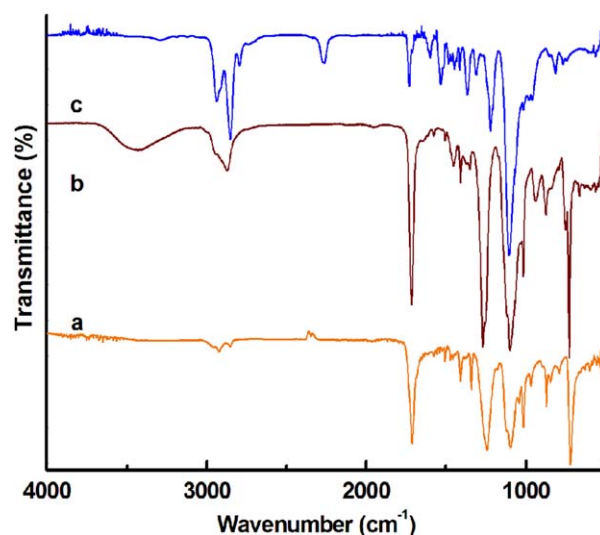


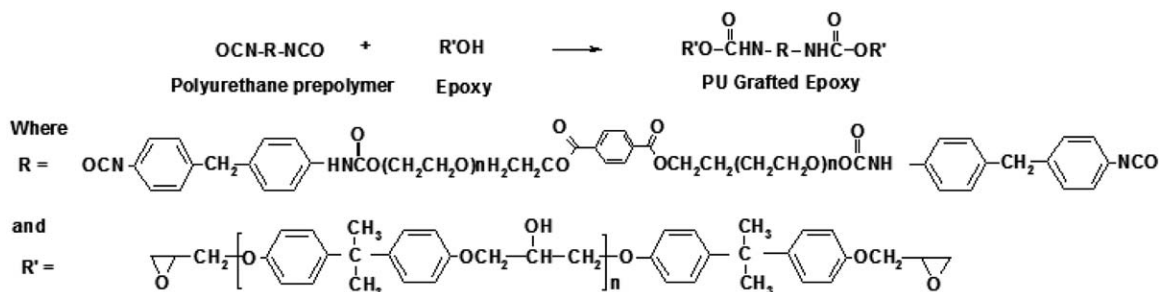
Figure 1. FTIR spectra (a) PET, (b) PY 1000, (c) PU 1000. [Color figure can be viewed in the online issue, which is available at wileyonlinelibrary.com.]

stretching (ν_{NCO}). The intensity of the hydroxyl band (~3200–3600 cm^{-1}) was substantially lower in the PU prepolymer, which is expected on the basis of its reaction with isocyanates.

Epoxy-Polyurethane Blends

Graft interpenetrating network of epoxy with polyurethane prepolymer was prepared by reacting the terminal NCO functionalities with the pendant hydroxyl groups available with the DGEBA-based epoxy resin to form polyurethane linkages (Scheme 2). In addition to increased interpenetration due to grafting, the possibility of hydrogen bonding between the hydroxyl groups in cured epoxy with the $>\text{C}=\text{O}$ groups of both carbamate and ester groups in polyurethane is expected to render improved mechanical strength to these blends.

It is to be noted that the uncured epoxy resin and polyurethane prepolymer were completely miscible under the experimental conditions employed, thereby forming a clear solution. The progress of this reaction was monitored by following the decrease in the intensity of the absorption band peaking at 2200 cm^{-1} (Figure 2). The NCO content was also determined by titrimetry and the decrease in the NCO indices is also presented in the figure. As expected, the intensity of the epoxide group stretching vibrations at 920 cm^{-1} remained unaltered, which clearly reveals the availability of these groups for subsequent curing



Scheme 2. Schematic representing the formation of epoxy-polyurethane graft interpenetrating networks.

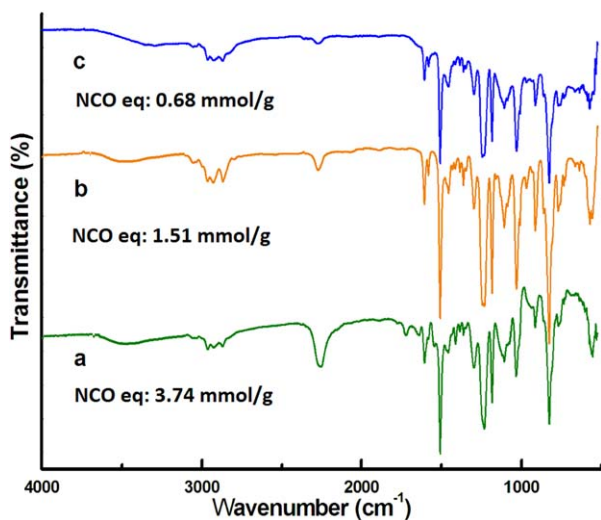


Figure 2. Changes in the FTIR spectra and NCO index due to grafting reaction of polyurethane with epoxy (E5PU1000) (a) 2 min, (b) 6 min, and (c) 10 min. [Color figure can be viewed in the online issue, which is available at wileyonlinelibrary.com.]

reaction. The resin was cured with TETA hardener after leveling of the isocyanate index (~ 10 min), which was allowed to continue for 24 h under ambient conditions.

The gel content of cured compositions was determined in order to quantify the extent of insolubility, which in turn is dependent on the extent of grafting and crosslinking. All the samples exhibited complete insolubility, as evidenced by high gel content $\sim 98.5 \pm 1\%$, irrespective of the amount and type of polyurethane used in the formulation, which confirms the formation of completely insoluble graft-interpenetrating networks.

Mechanical Properties

The effect of increasing the extent of polyurethane loading and chain length on the mechanical properties of the graft IPNs is presented in Figure 3 and the data is also tabulated in the Supporting Information Table S1. It can be seen that both tensile strength and impact toughness increased significantly due to introduction of polyurethane, which can be attributed to the increased level of interpenetration occurring as a consequence of

grafting reaction.²⁰ In addition, the intermolecular hydrogen bonds between the hydroxy groups available in cured epoxy with the carbonyl group of urethane and ester, are also expected to contribute significantly to the energy absorption characteristics of the polymer. Of all the formulations studied, maximum improvement was observed in blends prepared with polyurethane loading of 10% w/w (E10PU1000) which resulted in 61% increase in tensile strength and 212% increase in impact strength.

Earlier studies have revealed that blending of epoxy with poly(oxyethylene) (PEG 400)-based polyurethane led to 60% improvement in the impact strength,¹⁵ while in a separate study introduction of polyurethane (40% w/w) reportedly increased the impact toughness by 46%.³³ In comparison, the improvement in impact strength is larger (190%) when poly(oxypropylene)-based polyurethanes are blended with epoxy. Interestingly, blending of epoxy with polyester polyurethanes leads to larger improvements in impact strength (200%),¹⁷ as compared with polyether polyurethanes¹⁵ which may be attributed to the additional sites of hydrogen bonding available with the former. However, irrespective of the type of polyurethane being blended, the main cause behind the toughened nature of blends is the elastomeric nature of the polymer. The introduction of this rubbery phase hinders the process of crack propagation in the brittle epoxy matrix.¹⁵ The decrease in properties at higher loadings ($>10\%$), can be attributed to the formation of large separated phase domains at higher loadings.¹⁷

The flexural stress–strain response of neat epoxy has been compared with that of its blends with polyurethane in Figure 4. As expected, the graft IPNs exhibited higher flexural strength and high level of extensibility as compared with unmodified epoxy. More importantly, the graft-IPNs could be flexed to a higher extent and results in the yielding of the matrix prior to fracture, which in turn reflected in larger values of fracture toughness (K_{IC}). The load-deflection curve for notched specimens is also presented in Figure 4 (Inset), which clearly reveal the detrimental effect of notch on the flexural strength, which in turn can be attributed to stress concentration resulting from the reduced cross-sectional area.

A comparison of critical stress intensity factor (K_{IC}) and fracture energy (G_{IC}) as a function of polyurethane loading is presented in Figure 5. The stress intensity factor K_{IC} of epoxy

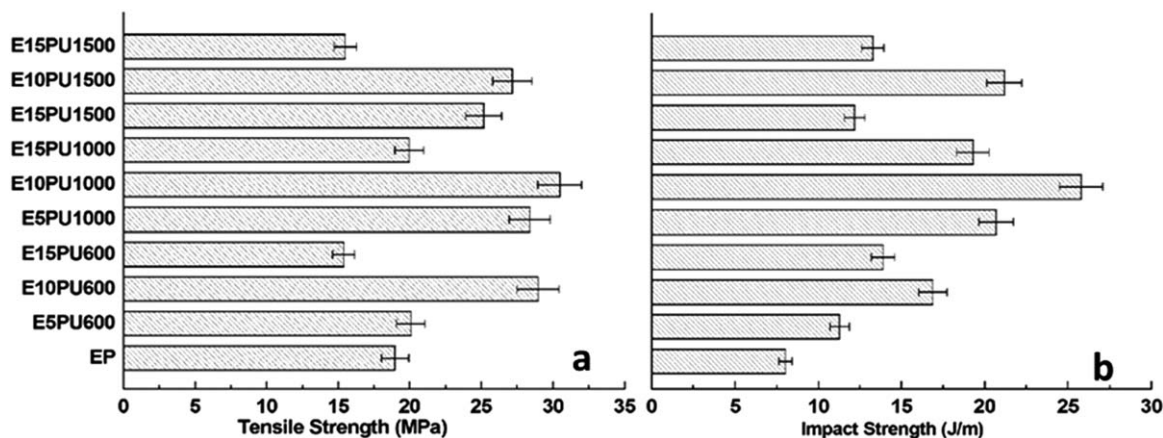


Figure 3. Improvement in mechanical properties of epoxy due to formation of graft IPN (a) Tensile Strength (b) Impact toughness.

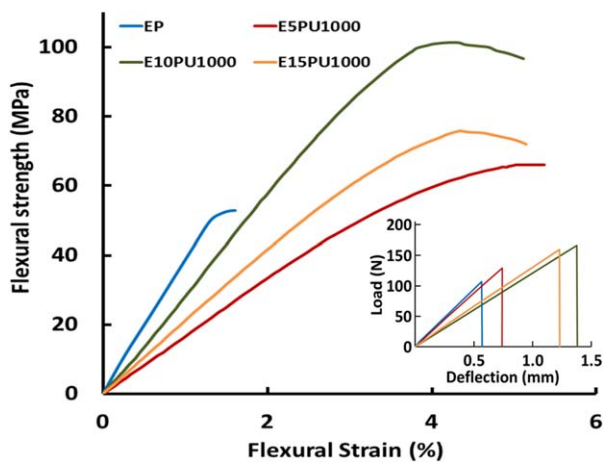


Figure 4. Representative stress–strain curves of epoxy and its blends with graft IPN with polyurethanes (flexural mode). Inset shows the effect of notch on the flexural response of specimens. [Color figure can be viewed in the online issue, which is available at wileyonlinelibrary.com.]

increased on blending, from an initial value of $2.18 \text{ MPa m}^{1/2}$ (unmodified) to $3.18 \text{ MPa m}^{1/2}$ for E10PU1000, which corresponds to an increase of $\sim 45.8\%$. The K_{IC} values were further used to calculate the fracture energy, which too was found to increase substantially, from a mean value of $4.29 \pm 0.4 \text{ kJ m}^{-2}$ (unmodified epoxy) to $12.2 \pm 0.4 \text{ kJ m}^{-2}$ after blending with 10% PU 1000 (184% increase). Our studies clearly bring out the potential of PET glycolysate-based polyurethane in the field of epoxy toughening.

Thermal Properties

The DSC traces of the cured epoxy and the graft networks formed with PU1000 are presented in Figure 6. The change in the baseline of the DSC trace of cured epoxy resin at $\sim 106^\circ\text{C}$ is associated with the reversible glass-rubber like transition of the amorphous epoxy structure, corresponding to the glass transition temperature (T_g) of the neat resin. It is to be noted that the reported T_g is just a convenient numerical representation of the entire glass

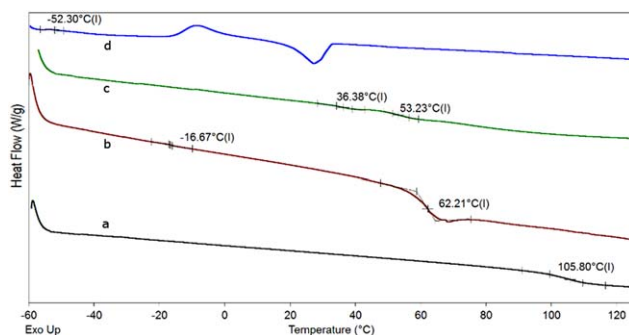


Figure 6. DSC traces of cured samples (a) neat epoxy, (b) E10PU1000, (c) E15PU 1000, and (d) PU 1000. [Color figure can be viewed in the online issue, which is available at wileyonlinelibrary.com.]

transition region. For comparison purposes, DSC analysis of cured polyurethane (PET glycolysate : NCO::1 : 1) was also performed, which revealed that the neat polyurethane exhibits elastomeric nature with a glass transition at -53°C followed by cold crystallization and melting. It is apparent from the figure that the glass transition region corresponding to the PU in the graft IPN shifts towards higher temperature, while that of epoxy is lowered, with the extent of shift being proportional to the amount of polyurethane blended, a feature characteristic of a partially miscible blends. Interestingly, epoxy-PEG graft IPNs have been reported to exhibit a single T_g characteristic of completely miscible blends.³⁴ The partial miscibility observed in this study can be attributed to the aromatic groups present in the PU segment, which results in phase separation.

The TG trace of epoxy and its graft IPN with polyurethane (PU 1000) is presented in Figure 7 and the data is tabulated in Supporting Information Table S2. The degradation behavior of epoxy resins have been extensively studied by several researchers,³⁵ and a two-step degradation process is generally reported. The first step is associated with evolution of water at $T > 100^\circ\text{C}$, followed by the pyrolytic decomposition of the main chain at $\sim 350^\circ\text{C}$, leading to the formation of condensable like acetone,

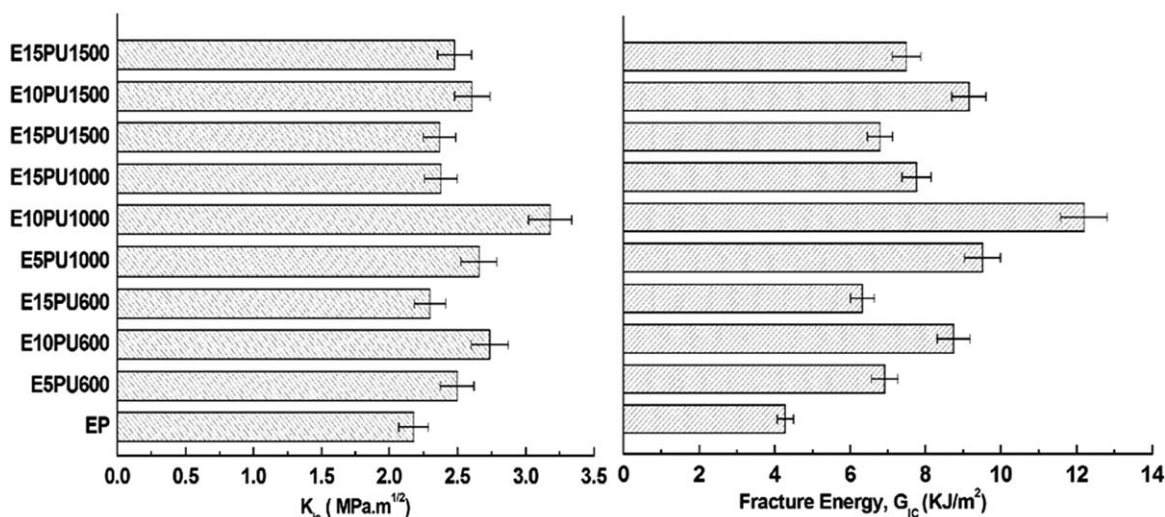


Figure 5. Improvement in fracture toughness (K_{IC}) and fracture energy (G_{IC}) of epoxy due to formation of graft IPNs.

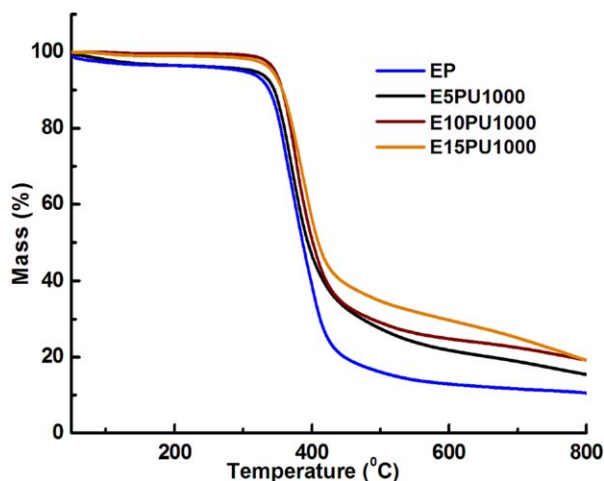


Figure 7. TGA trace of epoxy and its graft IPNs with polyurethane. [Color figure can be viewed in the online issue, which is available at wileyonlinelibrary.com.]

carbon dioxide, hydrogen cyanide, aliphatic hydrocarbons, etc.³⁵ The graft IPNs exhibit higher thermal stability in comparison to epoxy, which can be attributed to the presence of intermolecular hydrogen bonds between the hydroxyl group of epoxy and the carbamate group in polyurethane chain.³³ The IPNs also exhibited slightly higher char content as compared with the neat resin. However, the studies clearly established that all the compositions can safely be employed in service till 250°C, without any appreciable thermal degradation.

Morphological Studies

Fractographic analysis on the cracked surfaces was performed to gain an insight into the underlying micro-mechanisms behind the toughened nature of the graft IPNs. For this purpose, the fracture surface of both pristine epoxy and the interpenetrating networks were examined by SEM and the images are presented in Figure 8. As can be seen, the fracture surface of neat epoxy is almost featureless, indicative of uninterrupted crack propagation. Feather-like hackle markings could be observed on the surface of pristine epoxy, which changed into striations [Figure 8(a)] and finally transition to a mirror-like fracture surface.¹⁴ These surface features are characteristic of brittle failure, which in turn accounts for the low fracture toughness of neat epoxy.³⁶ Figure 8(b–d) presents the micrographs of fracture surfaces of the interpenetrating networks, which appear to be comparatively rough. The surface aberrations are clearly indicative of the significant amount of plastic deformation which occurs in the material prior to its ductile failure. Interesting features could be observed on the surface of IPNs at higher magnification. Evidence of rubber cavitation is presented in Figure 8(b–d), a mechanism which is most commonly cited to explain the toughened nature of rubber-epoxy blends. Tensile loading results in dilation of the plastic region surrounding the rubbery polyurethane phase, leading to its cavitation from within. The role of the cavitation process, therefore, is to relieve the plane strain constraint from the surrounding matrix which permits significant amount of plastic deformation.³⁷

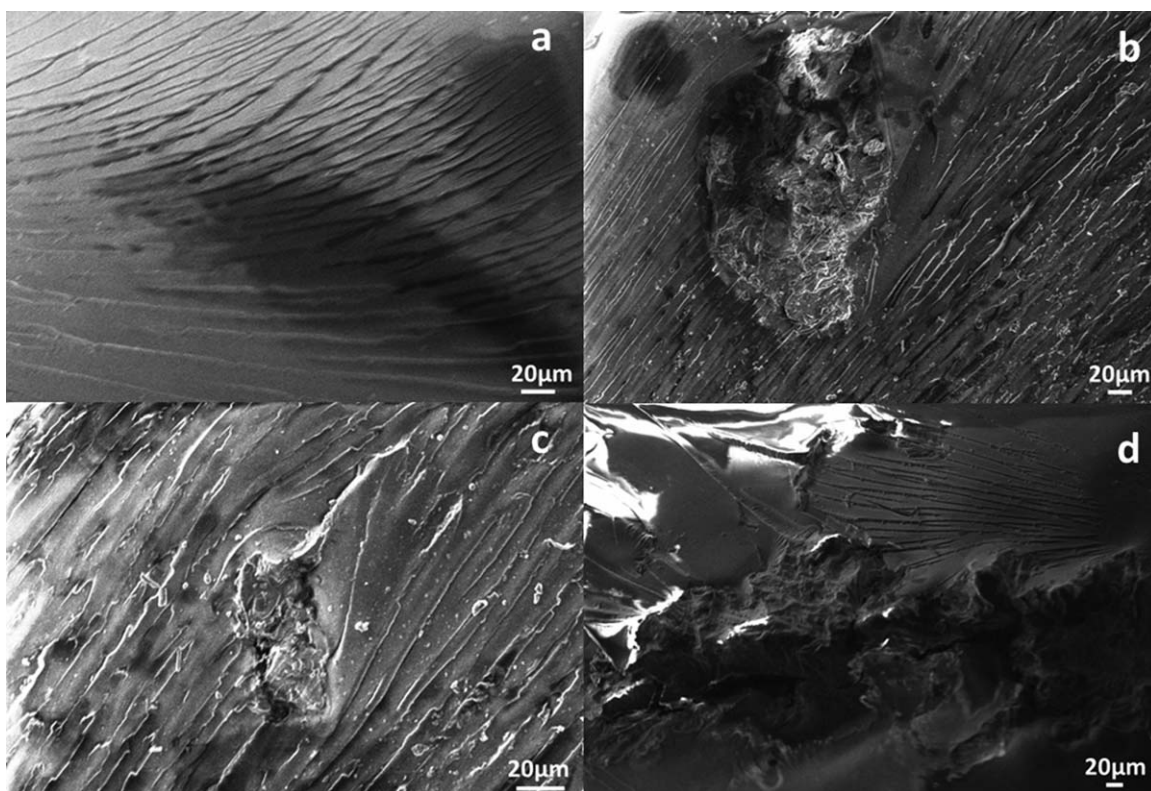


Figure 8. SEM images of fractured surface (a) neat epoxy, (b) E5PU1000, (c) E10PU 1000, and (d) E15PU 1000.

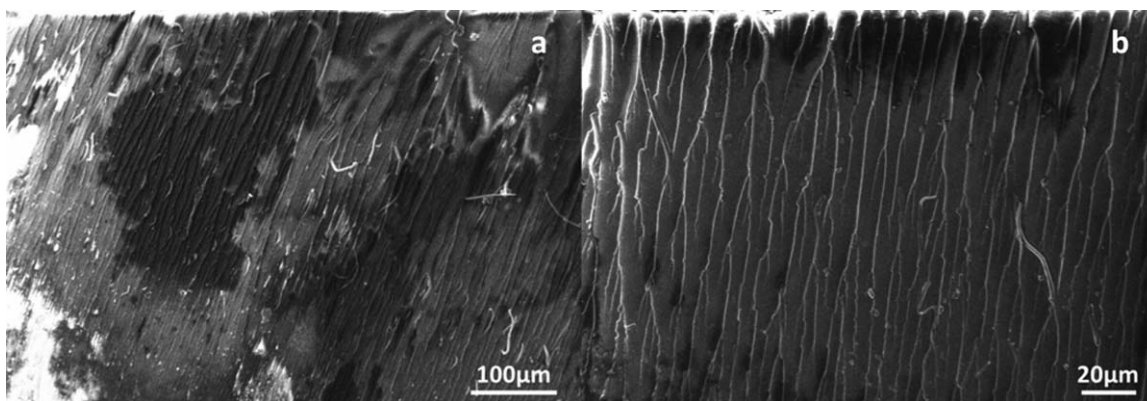


Figure 9. SEM images of fractured surface of E10PU1000 at different magnifications.

Another mechanism which can be used to explain the toughening in these toughened composites is that of particle yielding induced shear banding.³⁸ The process starts with the yielding of the polyurethane, thereby producing significant stress concentration, which in turn initiates shear banding in the matrix.

The rough texture of the fracture surface can also be attributed to crack path deflection and microcracking.³⁹ As a result of these phenomena, the surface area of the crack increases substantially and the mode I character of the crack opening is reduced, thereby resulting in increased energy for crack propagation. SEM micrographs at different magnifications are clearly indicative of this phenomenon (Figure 9).

CONCLUSIONS

PET was catalytically glycolysed with aliphatic polyethyleneglycols of varying molecular weight (600–1500) under microwave-assisted conditions. The resulting polyester polyols were reacted with MDI to form isocyanate terminated polyurethane prepolymer, which was subsequently blended with epoxy resin to form graft interpenetrating networks. The blends exhibited partially miscible nature, as indicated by two glass transition temperature with the shift in T_g being proportional to the amount of polyurethane being blended. The mechanical properties of the graft IPNs were studied under both quasi-static and dynamic conditions. In comparison to the neat resin, significant improvements in both tensile as well as impact strength were observed, the extent of which was dependant on the molecular weight of the polyurethane being introduced. Blending of epoxy with PU 1000 resulted in maximum improvement in the mechanical properties, with the improvement in impact properties being more pronounced (221% increase). As expected, the introduction of elastomeric polyurethane led to significant improvement in the fracture toughness, as indicated by flexure testing under single edge notch bending mode. The K_{IC} and G_{IC} values were found to increase by 46% and 184%, respectively as compared with neat resin. Morphological studies on the fracture surfaces was performed to gain an insight into the underlying toughening mechanisms. The unmodified epoxy fracture surface was featureless indicating brittle failure, while clear evidence of microcracking and rubber cavitation was observed on the fracture surface of the IPNs.

ACKNOWLEDGMENTS

The authors are thankful to Director, Centre for Fire, Explosive and Environment Safety, Delhi, India, for his keen interest in the work and providing logistic support to perform the study.

REFERENCES

- Welle, F. *Resour. Conserv. Recycl.* **2011**, *55*, 865.
- Bartolome, L.; Imran, M.; Cho, B. G.; Al-Masry, W. A.; Kim, D. H., Eds. *Recent Developments in the Chemical Recycling of PET*; InTech: Rijeka, Croatia, **2012**.
- Shen, L.; Worrell, E.; Patel, M. K. *Resour. Conserv. Recycl.* **2010**, *55*, 34.
- Lin, C. C. *Macromol. Symp.* **1998**, *135*, 129.
- Nikles, D. E.; Farahat, M. S. *Macromol. Mater. Eng.* **2005**, *290*, 13.
- Manju, P. K. R.; Ramanan, A.; Rajagopal, C. *Mater. Lett.* **2013**, *106*, 390.
- Awaja, F.; Pavel, D. *Eur. Polym. J.* **2005**, *41*, 1453.
- Vaidya, U. R.; Nadkarni, V. M. *J. Appl. Polym. Sci.* **1998**, *35*, 775.
- Vitkauskiene, I.; Makuska, R.; Stirna, U.; Cabulis, U. *J. Cell. Plast.* **2011**, *47*, 467.
- Abu Bakar, D. R.; Ahmad, I.; Ramli, A. *Malaysian J. Chem.* **2006**, *8*, 022.
- Kao, C. Y.; Cheng, W. H.; Wan, B. Z. *Thermochim. Acta* **1997**, *292*, 95.
- Chaudhary, S.; Parthasarathy, S.; Kumar, D.; Rajagopal, C.; Roy, P. K. *J. Appl. Polym. Sci.*, *131*, DOI:10.1002/app.39941 (2013).
- Chaudhary, S.; Surekha, P.; Kumar, D.; Rajagopal, C.; Roy, P. K. *J. Appl. Polym. Sci.* **2013**, *129*, 2779.
- Roy, P. K.; Mathur, R.; Kumar, D.; Rajagopal, C. *J. Env. Chem. Eng.* **2013**, *1*, 1062.
- Bakar, M.; Hausnerova, B.; Kostrzewa, M. *J. Thermoplast. Compos. Mater.* **2013**, *26*, 1364.
- Harani, H.; Fellahi, S.; Bakar, M. *J. Appl. Polym. Sci.* **1998**, *70*, 2603.
- Harani, H.; Fellahi, S.; Bakar, M. *J. Appl. Polym. Sci.* **1999**, *71*, 29.

18. Kostrzewa, M.; Hausnerova, B.; Bakar, M.; Dalka, M. *J. Appl. Polym. Sci.* **2011**, *122*, 1722.
19. Ong, S.; Ismail, J.; Bakar, M. A.; Rahman, I. A.; Sipaut, C. S.; Chee, C. K. *J. Appl. Polym. Sci.* **2009**, *111*, 3094.
20. Raymond, M. P.; Bui, V. T. *J. Appl. Polym. Sci.* **1998**, *70*, 1649.
21. Yeganeh, H.; Hojati-Talemi, P. *Polym. Degrad. Stab.* **2007**, *92*, 480.
22. Klinedinst, D. B.; Yilgör, I.; Yilgör, E.; Zhang, M.; Wilkes, G. L. *Polymer* **2012**, *53*, 5358.
23. Desai, S.; Thakore, I. M.; Sarawade, B. D.; Devi, S. *Eur. Polym. J.* **2000**, *36*, 711.
24. Huang, J.; Zhang, L. *Polymer* **2002**, *43*, 2287.
25. Rosu, D.; Rosu, L.; Varganici, C.-D. *J. Anal. Appl. Pyrolysis* **2013**, *100*, 103.
26. Wang, H.-H.; Chen, J.-C. *J. Appl. Polym. Sci.* **1995**, *57*, 671.
27. Yeganeh, H.; Lakouraj, M. M.; Jamshidi, S. *Eur. Polym. J.* **2005**, *41*, 2370.
28. Kostrzewa, M.; Hausnerova, B.; Bakar, M.; Siwek, E. *J. Appl. Polym. Sci.* **2011**, *119*, 2925.
29. Wang, H.; Liu, Y.; Li, Z.; Zhang, X.; Zhang, S.; Zhang, Y. *Eur. Polym. J.* **2009**, *45*, 1535.
30. Jog, J. P. *J. Macromol. Sci. Part C* **1995**, *35*, 531.
31. Knott, J. F. *Fundamentals of Fracture Mechanics*; Butterworths: London, **1976**.
32. Chen, J.; Kinloch, A. J.; Sprenger, S.; Taylor, A. C. *Polymer* **2013**, *54*, 4276.
33. Park, S.-J.; Jin, J.-S. *J. Appl. Polym. Sci.* **2001**, *82*, 775.
34. Varganici, C.-D.; Rosu, L.; Rosu, D.; Simionescu, B. C. *Compos. Part B: Eng.* **2013**, *50*, 273.
35. Vogt, J. *Thermochim. Acta* **1985**, *85*, 411.
36. Roy, P. K.; Ullas, A. V.; Chaudhary, S.; Mangla, V.; Sharma, P.; Kumar, D.; Rajagopal, C. *Iran. Polym. J.* **2013**, *22*, 709.
37. Bagheri, R.; Pearson, R. A. *Polymer* **2000**, *41*, 269.
38. Chen, T.; Jan, Y. *J. Mater. Sci.* **1991**, *26*, 5848.
39. Pearson, R. A.; Yee, A. F. *Polymer* **1993**, *34*, 3658.